Monte Carlo simulations of void-nucleated melting of silicon via modification in the Tersoff potential parameters

Paras Mal Agrawal,[1] Lionel M. Raff,[2] and Ranga Komanduri[1,*]
[1]*School of Mechanical and Aerospace Engineering, Oklahoma State University, Stillwater, Oklahoma 74078, USA*
[2]*Chemistry Department, Oklahoma State University, Stillwater, Oklahoma 74078, USA*
(Received 2 December 2004; revised manuscript received 11 May 2005; published 20 September 2005)

Molecular dynamics simulations of silicon melting reported in the literature using Tersoff's potential give melting temperatures about 50% higher than the experimental value. To address this discrepancy, we have proposed a modification to the values of the parameters of the Tersoff potential. This modification involves a change in the magnitude of 3 of the 12 parameters in the Tersoff potential as an effective means for bringing down the melting point close to the experimental value. The melting point is determined by performing Monte Carlo simulations using the empirical void-nucleated melting procedure. In addition to an agreement of the computed melting point with the experiment, the modified parameters also bring the density of the liquid and the solid at the melting point into good agreement with the experiment without significantly altering the density and energy values of the solid crystal at room temperature. The coordination number and specific heat of the liquid are also found to be in better agreement with the experiment when the modified set of parameters is used. A comparison of density over a wide range of temperatures shows that the density of the solid predicted by the Tersoff potential with the modified parameters is larger than that given by the unmodified parameters. This difference, however, is not appreciable at room temperature; it increases with temperature and is about 1% at the melting point. The computed cohesive energy of the solid, the point defect energy corresponding to a vacancy, and the surface energy values for (100) and (111) surfaces are also found to be nearly the same for the modified as well as the unmodified parameters.

DOI: 10.1103/PhysRevB.72.125206 PACS number(s): 34.20.Cf, 64.70.Dv, 65.20.+w, 65.40.−b

I. INTRODUCTION

The exploration of empirical intermolecular interaction potentials for a system of silicon atoms has been a subject of considerable interest.[1–22] One of the most popular potentials for silicon is the Tersoff potential.[1–4] It has been shown to explain various properties of silicon crystals. However, Cook and Clancy[23] have found, and Yoo *et al.*[24] have recently confirmed, that the Tersoff potential[4] predicts the melting point to be nearly 50% higher than experiment. This observation suggests the necessity of introducing some modification in the parameters of the Tersoff potential that will provide better agreement of the predicted melting point with experiment.

It is well known that molecular dynamics (MD) simulations of melting of a perfect crystal with periodic boundary conditions produce superheating due to the lack of free surface and defects. A large number of computational studies show that the mechanical melting temperature T_s at which a crystal without any defects and free surface melts is about 20% higher than the true thermodynamic melting point T_m. The ratio,

$$f = T_m/T_s \tag{1}$$

is found to be ~0.8 for a large number of systems. For example, the computed values of f for Ar over a wide range of pressure (0–53 GPa) is found to be 0.85 ± 0.03,[25–27] and in the range 0.77–0.81 for Ne,[28] Cu,[29] CH_3NO_2,[30] ammonium nitrate,[31] and ammonium dinitramide.[32] Using kinetic analysis of the homogeneous nucleation behavior for melting of superheated crystals, Lu and Li[33] found f in the range 0.82–0.85 for Ag, Al, Au, Co, Cu, Fe, Mn, Ni, Pd, Pt, and Sb, and lower values of f for metals with low melting points, i.e., 0.78 for Sn and 0.77 for Pb. It is, therefore, of interest to determine if the computed value of f for a covalent crystal, such as Si also falls in the same range.

Another point of interest in connection with the melting of silicon is the testing of an empirical method, namely, void-nucleated melting, for the determination of the melting point. The void-nucleated method for determining T_m is the result of empirical observations in various studies.[25–34] Detailed investigations of defect-nucleated melting of covalent and metallic solids have been reported by Phillpot *et al.*[34] and Lutsko *et al.*[29] The MD simulations of Lutsko *et al.* of a lattice containing nearly 1000 atoms of copper show that an ideal crystal melts at a temperature over 200 K above the thermodynamic melting temperature. Solca *et al.*[25,28] studied the void-nucleated melting method to determine the melting point of Ar and Ne. They noted that with the increase in the void size, the melting-temperature-versus-void-size curve first exhibits a decrease and then attains a plateau region that corresponds to the true melting temperature, and for a void size larger than that corresponding to the plateau region, the melting temperature plummets.

For Ar, at various values of pressure ranging from 0 to 53 GPa, Agrawal *et al.*[26] have confirmed this observation by comparing the melting point so determined with those computed by Zha *et al.*[35] using a thermodynamic method on the same potential. By simulating three types of voids in this study,[26] it has also been noted that melting temperature depends on the number of atoms removed and not upon the number of voids or the shape of the voids. In a

subsequent study on the melting of nitromethane, Agrawal *et al.*[30] obtained good agreement between the melting point computed from the plateau region in the melting-temperature-versus-void-size curve and that determined by the method based on the equilibration of a mixture of liquid and solid.[36]

Besides Ar, Ne, and CH_3NO_2, the void-nucleated melting method has also been tested for CH_3COOH,[37] cyclotrimethylene trinitramine (RDX),[38] 1,3,3-trinitroazetidine (TNAZ),[38] ammonium nitrate,[31] and ammonium dinitramide.[32] The method, however, is empirical in that there is no theoretical basis to validate the assumption that the melting temperature in the plateau region is the true melting point. Therefore, it may be interesting to see if this void-nucleated melting method is applicable for a covalent system, such as Si where we have the results of other studies[23,24] for comparison.

In this paper, we report the results of computations of the melting point of silicon using the Tersoff potential[4] and the void-nucleated method. The results provide additional information related to the validity of the void-nucleated method and the value of f for Si. In addition, the study results in a modification of the parameters of the Tersoff potential[4] that gives a melting point in agreement with experiment.

II. COMPUTATIONAL DETAILS

A. Force field

We have investigated the Tersoff potential,[4] which is expressed in terms of 12 parameters as follows:

$$V_{\text{Tersoff}} = (1/2)\sum_{i\neq j} V_{ij}, \tag{2}$$

where

$$V_{ij} = f_c(r_{ij})[A\exp(-\lambda r_{ij}) - b_{ij}B\exp(-\mu r_{ij})], \tag{3}$$

$$b_{ij} = \chi(1+\beta^n\zeta_{ij}^n)^{-1/2n}, \tag{4}$$

$$\zeta_{ij} = \sum_{k\neq i,j} f_c(r_{ik})g(\theta_{ijk}), \tag{5}$$

$$g(\theta_{ijk}) = 1 + c^2/d^2 - c^2/[d^2 + (h-\cos\theta_{ijk})^2], \tag{6}$$

and

$$f_c(r_{ij}) = \begin{cases} 1 & \text{for } r_{ij} < R, \\ \frac{1}{2} + \frac{1}{2}\cos[\pi(r_{ij}-R)/(S-R)] & \text{for } R < r_{ij} < S, \\ 0 & \text{for } r_{ij} > S. \end{cases} \tag{7}$$

The parameters of the potential, as given in Ref. 4 are listed in Table I.

For the purpose of discussion, we shall denote the above-mentioned potential as V_{IV} or the Tersoff-4 potential to distinguish it from other similar potential functions with different sets of parameters given by Tersoff.[1–3] We denote those given by Tersoff in Refs. 1–3 by V_{I}, V_{II}, and V_{III} or Tersoff-1, Tersoff-2, and Tersoff-3 potential, respectively. The notations, Tersoff-2 and Tersoff-3 are consistent with those used by Balamane *et al.*[39]

TABLE I. The modified and unmodified parameters of the Tersoff potential.

Tersoff parameters	Tersoff-4[a]	Tersoff-ARK
A (eV)	1.8308×10^3	1.8308×10^3
B (eV)	4.7118×10^2	4.7118×10^2
λ (Å^{-1})	2.4799	2.4799
μ (Å^{-1})	1.7322	1.7322
β	1.1×10^{-6}	$\mathbf{1.15\times10^{-6}}$
n	0.78734	**0.988**
c	1.0039×10^5	1.0039×10^5
d	16.217	16.217
h	−0.598 25	**−0.745 25**
R (Å)	2.7	2.7
S (Å)	3.0	3.0
χ	1.0	1.0

[a]Reference 4.

B. Monte Carlo simulations and melting

1. NPT simulations

Monte Carlo (MC) simulations at constant pressure (P) and constant temperature (T) for a fixed number of atoms (N) as described in Ref. 40 are performed to simulate melting. A $3\times3\times3$ supercell of Si crystal having 216 atoms has been considered. The cubic simulation box has an edge length of L. Periodic boundary conditions have been used. At every cycle during the MC walk, $N+1$ moves were attempted. These correspond to a random move of each of N atoms and a random change in the size of the simulation box. The coordinates and box size have been varied according to the following standard equations given in Ref. 40:

$$q_i(\text{new}) = q_i(\text{old}) + (2\xi_1 - 1)(\Delta q)_{\max}, \tag{8a}$$

$$L(\text{new}) = L(\text{old}) + (2\xi_2 - 1)(\Delta L)_{\max}, \tag{8b}$$

where ξ_1 and ξ_2 are random numbers chosen uniformly in the interval 0 to 1, and $(\Delta q)_{\max}$ and $(\Delta L)_{\max}$ are the maximum step sizes for the translation of the Cartesian coordinate (q) of an atom and box length (L), respectively. These maximum displacements have been determined to obtain an acceptance ratio of about 50% from the total number of attempted moves and their values were $(\Delta q)_{\max}=0.15$ Å and $(\Delta L)_{\max}=0.13$ Å.

A walk or a change made in the box size is accepted, if either $W<0$ or

$$\exp(-W/k_BT) > \xi, \tag{9}$$

otherwise the move is rejected. In the above relation, k_B is Boltzmann's constant, ξ is a random number chosen uni-

formly in the interval 0 to 1, and W is given by

$$W = P(v_{\text{new}} - v_{\text{old}}) + (V_{\text{new}} - V_{\text{old}}) + Nk_BT \ln(v_{\text{old}}/v_{\text{new}}). \tag{10}$$

Here, the subscripts new and old have the usual meaning, v denotes the volume of the box, V represents the total interaction energy of the system, and P and T signify the external pressure and temperature at which the calculations were made. When a move is rejected, the properties corresponding to the previous configuration were included in the averages. A new configuration was then generated from this previous configuration.

2. Creation of voids and gradual heating

Starting from the ideal configuration at $T=0$ K, an equilibrated configuration at $T=500$ K and $P=1$ atm is obtained by running 10 000 cycles of Monte Carlo simulations. By successive simulations, each for 10 000 cycles, the equilibrated configurations at temperatures 1000, 1500,…, and 3000 K have been obtained. All the simulations have been run at $P=1$ atm. From this set of configurations, the closest configuration at a temperature lower than T_o is simulated for 10 000 cycles to obtain an equilibrated configuration at temperature T_o. After equilibrating the system at temperature T_o, N_{void} atoms have been removed out of the total N_o atoms. The locations of these N_{void} atoms have been chosen randomly with the constraint that the minimum distance between any two is greater than $r_{\min}$, where $r_{\min}$ is chosen nearly as large as possible. We choose this number N_{void} to signify the void size.

After the creation of voids, this system of $N=N_o-N_{\text{void}}$ atoms is again equilibrated at temperature T_o and pressure P by running MC simulations for n_o cycles. The heating of the system from initial temperature T_o is achieved by uniformly changing the temperature by $\Delta T=0.001$ K, after each cycle of $N+1$ moves. Thus, the temperature at the nth cycle of moves is

$$T = T_o + (n - n_o)\Delta T. \tag{11}$$

The gradual heating of the system in the MC simulations has been achieved by redefining the desired temperature in Eqs. (9) and (10) during constant number-pressure-temperature (NPT) simulations. This method of gradual heating based on redefining the desired temperature in NPT simulations has also been employed earlier for the melting studies of Ar[26] and nitromethane[30] by MD simulations. The success of this procedure has been tested in those studies[26,30] by monitoring the temperature and pressure as a function of integration time; there it has been found that pressure remains constant and the temperature changes according to the desired input temperature. Here in MC simulations we do not have the kinetic energy to monitor the temperature, but we have tested the increase in temperature by monitoring the variation in the potential energy with the MC cycle number during the heating process. Figure 1 depicts this variation in the potential energy per atom with T given by Eq. (11) in a simulation corresponding to $T_o=1500$ K and $\Delta T=0.001$ K/cycle. Each point in the figure has been obtained by averaging the potential energy over 1000 cycles. The straight line in the figure corresponds to the least-squares fit. As expected, we note that the slope of the straight line is equal to $\frac{3}{2}k_B$ that shows that the system is being heated according to the temperature given by Eq. (11).

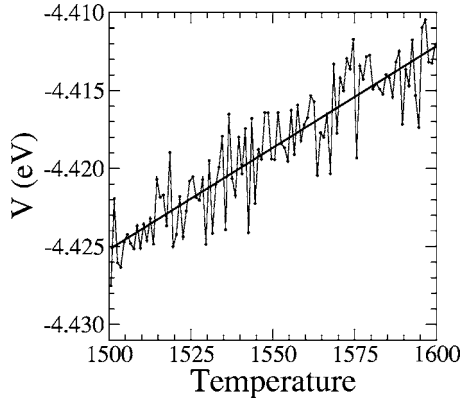

FIG. 1. Variation of potential energy per atom as a function of temperature T given by Eq. (11). The straight line shows the least squares fit.

3. Order parameter

The melting of the system has been identified by monitoring the energy and the order parameter (ζ)[26,30] as a function of temperature during the heating process. At the melting temperature, these parameters change abruptly. Since the diamond structure can be considered as a combination of two fcc structures, we can write ζ as an average of the order parameters of the two structures, i.e.,

$$\zeta = \frac{1}{2}\sum_{i=1}^{2} \zeta_i, \tag{12}$$

where

$$\zeta_i = (1/N_c)\left| \sum_{j=1}^{Nc} \exp(i\mathbf{k}\cdot\mathbf{r_j}) \right|. \tag{13}$$

In these equations $N_c \approx N/2$, $\mathbf{r_j}$ is the position vector of the jth atom of ith fcc structure and $\mathbf{k}$ is the reciprocal lattice vector. For the fcc lattice,[26,40]

$$\mathbf{k} = (2\pi/a_o)(-1,1,-1), \tag{14}$$

where a_o is the length of the unit cell. It is trivial to see that for an ordered crystal $\zeta \to 1$ and $\zeta \to 0$ for the liquid state.

C. MD simulations

We employed a larger system, a $5\times5\times5$ supercell of Si having 1000 atoms, to compute density, configurational energy, specific heat, coordination number, and radial distribution function. Such a system has been simulated using isothermal-isobaric molecular dynamics (NPT-MD) method. The Melchionna modification[41] of the Nosé-Hoover equations of motion was used to achieve the constant temperature and pressure. The thermostat, as well as barostat relaxation

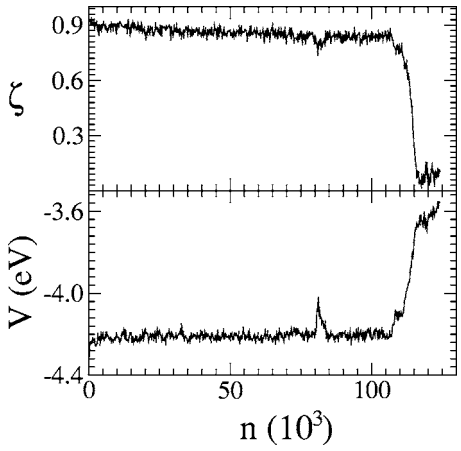

FIG. 2. Variation of order parameter (ζ) and potential energy per atom (V) as functions of Monte Carlo simulation cycle number (n) for the Tersoff-4 potential with initial temperature (T_o)=2950 K, void size (N_{void})=0, and $n_o=10\times10^3$ cycles.

time, has been chosen as 50.0 t.u. (1 t.u.$=1.018\times10^{-14}$ s), and the Verlet leapfrog procedure[40] (with time step 0.05 t.u.) has been used to integrate the equations of motion. Computed results are given in Figs. 7–9 and Tables III and V.

III. RESULTS

A. Melting

Figure 2 shows the variation of order parameter ζ and the configurational energy per atom V as a function of the Monte Carlo cycle number n for a system of 216 atoms at P =1 atm initially at temperature T_o=2950 K with no voids. The heating according to Eq. (11) has been started after n_o =10 000 cycles. A rapid change in ζ and V depicted by these curves at $n=107\times10^3$ cycles corresponds to the melting at T=3047 K.

Figure 3 gives the variation of the transition temperature as a function of the void size, N_{void}, defined by the number of atoms randomly removed from the crystal. Multiple points at a value of N_{void} in the figure demonstrate the effect of varying either the initial phase or temperature of the system. This figure shows that the transition temperature decreases as N_{void} increases. A horizontal line in the figure has been drawn to mark the average temperature in the plateau region corresponding to $11\leqslant N_{\text{void}}\leqslant14$. The average temperature in this region is 2509±44 K. With the assumption that the transition temperature in the plateau region is the melting temperature that corresponds to the thermodynamic melting point, we obtain 2509 K as the melting point given by this void-nucleated method, which is in good agreement with the computed values, 2567 K and 2584 K, given by Yoo *et al.*[24] using the same potential and the method of coexisting solid-liquid phases and 2547±22 K given by Cook and Clancy.[23]

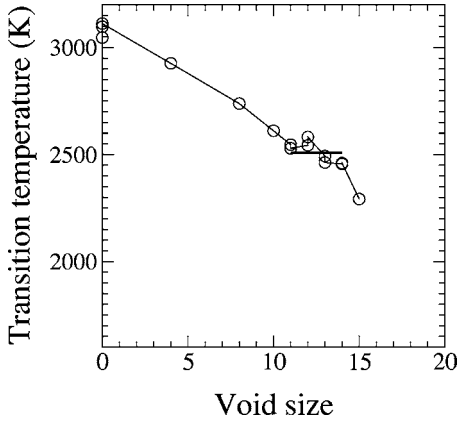

FIG. 3. Transition temperature as a function of the void size (N_{void}) for the Tersoff-4 potential. The horizontal line shows the average temperature (2509 K) in the plateau region.

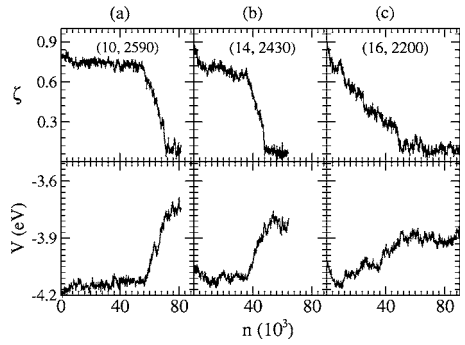

FIG. 4. Same as Fig. 2, but for different values of void size (N_{void}) and initial temperature (T_o): (a) N_{void}=10, T_o=2590 K; (b) N_{void}=14, T_o=2430 K; (c) N_{void}=16, T_o=2200 K.

A few typical curves showing the variation of order parameter (ζ) and configurational energy (V) for N_{void}=10, 14, and 16, respectively, are shown in Figs. 4(a)–4(c). For all these curves, n_o=10 000 cycles and T_o values are 2590, 2430, and 2200 K, respectively, as indicated in the figure. A comparison of the curves corresponding to N_{void}=14 and 16 shows that melting point decreases from 2456 K for void size N_{void}=14 to less than 2200 K for void size N_{void}=16.

For the sake of further discussion, following the previous studies,[25,26,28,30] we introduce a term, "critical void size," to refer to the maximum value of the void size in the plateau region. It may be noted that the critical void size depends on the substance, the interaction potential function, pressure, and the number of atoms (N) considered in the simulation box. For example, the studies of Agrawal *et al.*[26] on the melting of Argon reveal that at a given pressure (P =44.56 kbar) the critical void size increases from 50 to 120 as N increases from 864 to 2040.

In view of various simulation studies on Ar, Ne, CH_3NO_2, RDX, TNAZ, ammonium nitrate, and ammonium dinitramide, it is not surprising to note that the value of the melting point of Si given by the void-nucleated method employed here agrees with the previously reported[23,24] melting point values.

However, one needs to make a rigorous analysis of the appropriateness and limitations of this method. Due to the lack of understanding of the mechanism of melting, the relationship between the existence of the above-mentioned plateau region and the mechanism of melting is not yet known. There have been various studies to explore the mechanism of melting. The Lindemann criterion[42] of melting and the Born

TABLE II. A comparison of melting temperatures given by the modified (V_V) and unmodified (V_{IV}) Tersoff potential parameters with the experiment.

	T_s (K)	T_m (K)	$f=T_m/T_s$
Tersoff-4[a]	3075±29	2509±44	0.82
Tersoff-ARK[b]	2097±21	1711[c]	
Experiment		1687[d]	

[a]Reference 4.
[b]Present modification.
[c]Obtained by using Eq. (1) and $f=2509/3075$.
[d]Reference 49.

instability criterion[43] of melting have been of importance in explaining the mechanism of melting. The investigations of Jin *et al.*[27] show a strong correlation between the Lindemann and the Born instability criteria. The Lindemann criterion based on the mechanical approach of melting has gained more attention as a result of the recent investigations of Burakovsky *et al.*[44] regarding the melting of elements based on the dislocation mechanism.[44–47] Considering melting as a dislocation-mediated phase transition, Burakovsky *et al.*[44] computed melting curves for 24 elements in good agreement with the available data. They also note that their dislocation-based melting approach leads to melting points that are very close to those given by the Lindemann criterion. Gomez *et al.*[47] showed that defects which occur in the solid phase as the transition temperature is approached are responsible for melting. However, we are still in the learning phase in the area of the mechanism of melting. One would like to rigorously learn if the existence of the plateau region in the void-size-versus-melting-temperature curve is universal and whether the melting point in the plateau region corresponds to the thermodynamic melting point.

B. Superheating and *f* factor

The extent of superheating of a crystal can be measured by the ratio f given by Eq. (1). Table II gives the value of the melting point without any void, $T_s=3075$ K, determined by averaging over four values of the computed melting points with different initial conditions. The true or thermodynamic melting temperature $T_m=2509$ K given by the average of the melting temperatures in the plateau region, as discussed in Sec. III A, leads to $f=0.82$.

It is interesting to note that this value of $f=0.82$ for a covalent Si crystal is comparable to that determined by the homogeneous nucleation model of Lu and Li[33] for Al, Au, Co, Cu, Fe, Mn, Ni, Pb, Pd, Pt, Sb, and Sn, and those computed for Ar, Ne, Cu, CH_3NO_2, RDX, TNAZ, ammonium nitrate, and ammonium dinitramide. For all these crystals f is found to be in the range 0.77 to 0.85.

A near constant value of f for a large number of systems suggests the possibility of $f\sim0.80$ for many other substances. Thus, the prediction of f in this range may be an important criterion to judge the validity of a theoretical model. Further, the rigorous determination of f by some theoretical model would also make the determination of T_m easy.

As regards the effect of the size of the simulation box on the factor f that signifies the degree of superheating, Agrawal *et al.*[26] have found that the value of f for a system of argon crystals does not change when the periodic system containing 864 atoms is replaced by that having 2048 atoms. A simulation of 6912 atoms of Ar by Jin *et al.*[27] also gave almost the same value of f. The agreement between the computed values of f and those given by Lu and Li[33] as discussed in the above paragraphs also suggest the possibility of insignificant change in the value of f as the number of atoms in the periodic system considered is increased by a large extent. Also, based on the Lindemann criterion,[42] namely, a solid melts when the amplitude of atomic vibrations exceeds a certain fraction of the lattice spacing, it appears that the melting temperature or superheating of an ideal crystal with the periodic boundary conditions would not change when the system size is increased although the limits of this generalization have not been established.

C. Modification in the potential

1. Addition of long-range interactions

In the Tersoff potential, $f_c(r_{ij})$ occurring in Eq. (3) is assumed to be zero for $r_{ij}>3.0$ Å for a silicon crystal. To examine the effect of long-range interaction, we have added a Lennard-Jones (12-6) interaction,

$$V_{LJ}(r_{ij}) = 4\varepsilon[(\sigma/r_{ij})^{12} - (\sigma/r_{ij})^{6}], \tag{15}$$

to the Tersoff potential V_{IV} and then determined the melting point. The values of parameters, $\sigma=3.826$ Å and $\varepsilon=0.017\,44$ eV have been taken from Refs. 48 and 49. To avoid strong repulsions due to this term, we considered this interaction only when $r_{ij}>4.0$ Å.

By running a Monte Carlo simulation with the addition of such a long-range interaction, we found that melting occurs at 3116 K when void size=0. If we compare this value of T_s with $T_s=3075\pm29$ K, given by the Tersoff-4 potential alone, we infer that the effect of the addition of van der Waals interactions in the Tersoff potential on the melting is very small. Therefore, we need to look for some more significant modification to obtain a melting point in agreement with the experiment.

2. Choice of new parameters

After running a few sets of simulations by varying the magnitude of 3 of the 12 parameters in the Tersoff potential, it has been observed that a combination of β, n, and h parameters occurring in Eqs. (4) and (6) would give values of the melting point and density of liquid Si in agreement with experiment without introducing appreciable change in the density and configurational energy of a solid Si crystal at low or room temperatures. We have not attempted any change in parameters A, B, λ, μ, and χ as the properties of the solid even at low temperatures may be very sensitive to these parameters. Similarly, we did not investigate the effect of varying R, S, c, and d as these parameters may not be as effec-

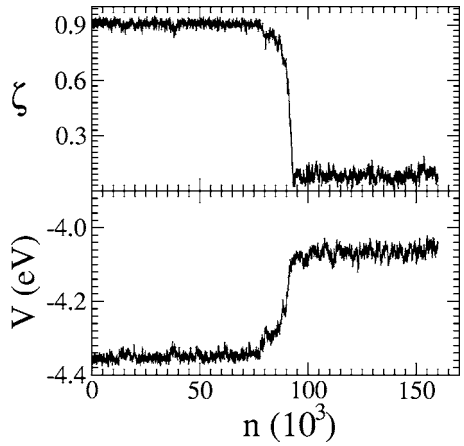

FIG. 5. Variation of order parameter (ζ) and potential energy per atom (V) as functions of Monte Carlo simulation cycle number (n) for Tersoff-ARK potential with initial temperature (T_o)=2000 K, void size (N_{void})=0, and $n_o=10\times10^3$ cycles.

tive, in modifying the melting point as well as the density of liquid without introducing appreciable changes in the density and cohesive energy of the solid at low or room temperatures, as β, n, and h. To achieve this, we first tested various combinations of n and h in a coarse grid without changing the value of β. The values of n and h ranging from ~0.75 to 1.5 times their original values have been attempted to reproduce the melting point. A finer grid of β, n, and h is then explored to reproduce the melting temperature, liquid density, and cohesive energy of the solid. The values of β, n, and h so determined are 1.15×10^{-6}, 0.988, and −0.745 25, respectively (see Table I). For further discussion, let us denote the Tersoff potential with these modified parameters as V_{V} or Tersoff-ARK (Agrawal-Raff-Komanduri) potential. The results obtained with Tersoff-ARK are discussed in Secs. III C2*a*–III C2*e*.

a. Melting point. Similar to the results shown in Fig. 2 for the Tersoff-4 potential, we get Fig. 5 for the Tersoff-ARK potential. In this simulation T_o=2000 K, n_o=10 000 and, melting occurs at n=79 000 that correspond to melting at 2069 K for a crystal without any void. Figures 6(a)–6(i) show the configurations of the system of 216 silicon atoms at various stages of this simulation. Figures 6(a)–6(c) depict the crystalline phase. Figure 6(d) corresponds to n=79 000 when the crystal starts melting and the order parameter (ζ) just begins to drop (see Fig. 5 for n versus ζ curve for this simulation). Figures 6(e) and 6(f) exhibit the configurations at n =85 000 and 90 000, respectively; these belong to the region of the rapid drop in the order parameter (see Fig. 5). Figures 6(g)–6(i) represent configurations at n=95 000, 100 000, and 105 000, respectively; this region corresponds to the liquid characterized by low values of the order parameter (see Fig. 5).

By averaging the results on a set of four such simulations with different initial conditions, we get the mechanical melting temperature as $T_s=2097\pm21$. Using Eq. (1) and assuming the value of $f=T_m/T_s=2509/3075$, as described in Sec. III B, we obtain the melting temperature, T_m=1711 K (see Table II), which is in good agreement with the experimental value 1687 K.[49]

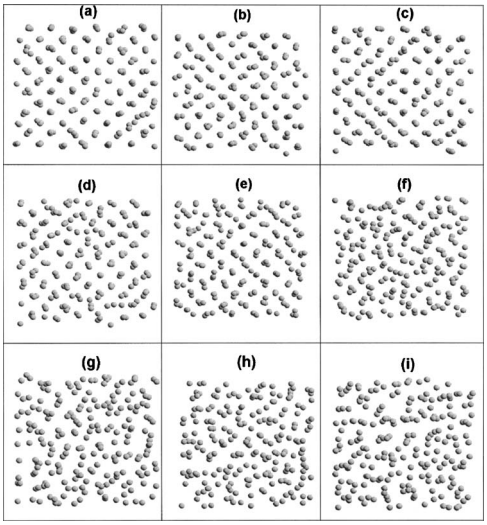

FIG. 6. The configuration of silicon atoms at various stages of a MC simulation at n=(a) 1000, (b) 40 000, (c) 75 000, (d) 79 000, (e) 85 000, (f) 90 000, (g) 95 000, (h) 100 000, and (i) 105 000 for Tersoff-ARK potential with initial temperature (T_o)=2000 K, void size (N_{void})=0, and $n_o=10\times10^3$ cycles.

b. Density. Figure 7 compares the density of a solid and a liquid for the Tersoff-ARK (solid curve) and the Tersoff-4 (dotted curve) potentials. We note that at low temperatures, the densities of the solids given by V_{IV} and V_{V} are in excellent agreement. However, the density values predicted by V_{V} are found to be larger than those given by V_{IV} at higher temperatures. The difference increases with temperature. At the melting point, this difference is about 1%. For the liquid, we see a large difference in the densities predicted by these two potentials. At 1687 K, the density of liquid predicted by V_{V} is found to be 2.589 ± 0.013 g cm^{-3}, which is in excellent agreement with the experimental density 2.583 g cm^{-3}.[50] V_{IV}, however, gives a density of 2.225 g cm^{-3} for the supercooled liquid at this temperature. It may be noted that for the Tersoff-ARK potential at 1687 K, the ratio, $\Delta V/V_s$, of change in volume Δv to the volume of solid V_s at the phase transition is equal to −11.8%, which is in excellent agreement with the experimental value −11.9%.[51]

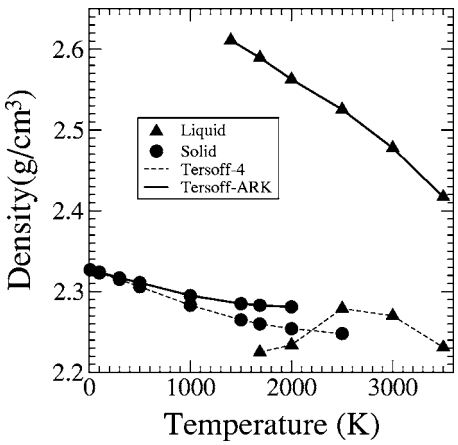

FIG. 7. The variations in densities of solid (●) and liquid (▲) as a function of temperature: solid curves for Tersoff-ARK potential and dotted curves for the Terosoff-4 potential.

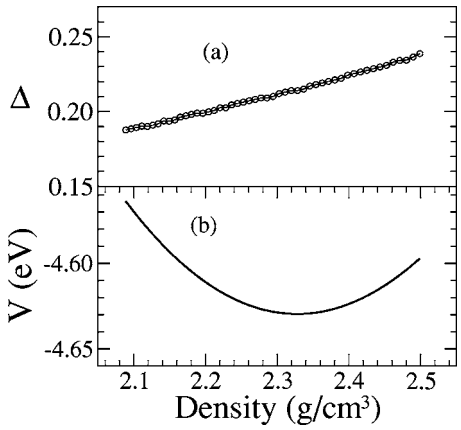

FIG. 8. (a) The difference in energy Δ as defined by Eq. (16); (b) the value of the configurational energy per atom, as a function of density for silicon in the ideal tetrahedral configuration at $T=0$ K.

c. Energy. We have compared configurational energy of Si in the solid phase in two ways: (i) At $T=0$ for different values of pressure or density, and (ii) at $P=0$ for different values of temperatures. In Fig. 8(a), we have shown the difference in the two potentials by a parameter Δ defined as

$$\Delta = 10^5(V_V - V_{IV})/V_{IV}, \tag{16}$$

where V_V and V_{IV} are computed for an ideal tetrahedral geometry at $T=0$ at different values of pressure, which can be specified by the density of the crystal. We note that for $\Delta < 0.25$, i.e., the two potentials differ by less than 0.000 25% over a wide range of pressure, at $T=0$. In this connection, it may also be interesting to see the behavior and absolute value of V_V per atom in this configuration; Fig. 8(b) gives these data.

Figure 9 compares the configurational energy given by the two potentials at various temperatures. It shows the variation of configurational energy per atom as a function of temperature for Si in solid and liquid phases for the Tersoff-ARK (solid curve) and the Tersoff-4 (dotted curve) potentials at $P=0$. In the case of the solid, the results of V_{IV} and V_V differ

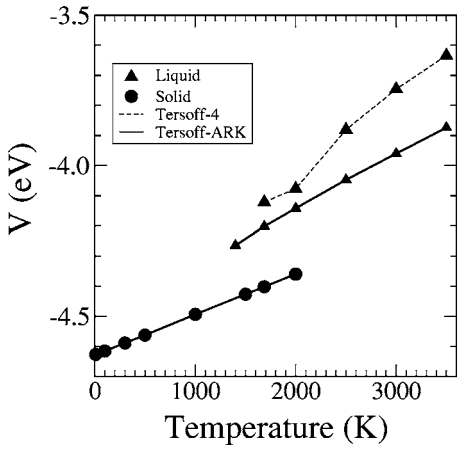

FIG. 9. The configurational energy values of solid (●) and liquid (▲) as functions of temperature: solid curves for the Tersoff-ARK potential and dotted curves for the Terosoff-4 potential.

by less than 0.001 eV and, therefore, the dotted curve corresponding to the potential V_{IV} coincides with the solid curve. The slope of the kinetic-energy-versus-temperature curve for the classical model is trivially 1.5 k_B. By summing the slope of the potential and kinetic energies, we can obtain the specific heat C_p. It is interesting to note that in this classical simulation, the average slope of the potential energy curve for the solid is nearly equal to that given by the kinetic energy curve. The average value of C_p in the temperature range 100–2000 K for the Tersoff-ARK potential as well as the Tersoff-4 potential is found to be 25.4 J mol^{-1} K^{-1}, which is in good agreement with the experimental values[52] at high temperatures: 25.359, 27.196, and 28.870 J mol^{-1} K^{-1} at $T=800$, 1200, and 1600 K, respectively.

As shown in Fig. 9, in the case of the liquid, we note a large difference between the configurational energy values given by the two models. We also note significant variation in the slopes with temperature. With respect to the average specific heat in the range 1687 to 2000 K, we obtain $C_P = 31.0$ J mol^{-1} K^{-1} for V_V, that given by V_{IV} in the temperature range 2500–3000 K is 38.5 J mol^{-1} K^{-1}, against the experimental value of 29.2 J mol^{-1} K^{-1} at $T=1687$ K (see Table III).

From the information given in Fig. 9, we can determine the heat of fusion as 19.3 kJ mol^{-1} for the Tersoff-ARK potential, which is in poor agreement with the experimental value,[53] 50.6 kJ mol^{-1} (see Table III). This disagreement suggests the need for further improvement in the potential.

Using MD simulations, the configurational energy (V) as well as the density for a liquid and a solid at various temperatures have also been computed using the Tersoff-ARK potential on the periodic system having 216 atoms in the simulation box. The computed values so obtained are found to be in excellent agreement with the corresponding values reported in Figs. 7 and 9 for the periodic system having 1000 atoms. Regarding the size dependence of the computed melting point, Miranda and Antonelli[60] recently reported an agreement between the values of the melting point of silicon given by the periodic systems having 216 and 512 atoms in the simulation box. From the results presented here, together with the other results available in the literature, it appears that the values of the melting point, density, and configurational energy determined in the present studies are size independent, at least in the range of atoms considered; although, the limits of this generalization have yet to be established. Whether or not the degree of overheating of the periodic system with an extremely large number of atoms (say on the order of a billion or more) would change due to the change in the lattice vibrations remains to be seen. Admittedly, simulations of such large systems require very fast, highly powerful computers with adequate memory. The availability of such systems (single systems or with parallel processing capability) in the not too distant future can answer this question more definitely.

d. Point defect and surface energies. In Table IV, we have reported the computed values of the point defect and surface energy values given by the Tersoff-4 and Tersoff-ARK potentials for vacancy, hexagonal interstitial, and tetrahedral interstitial defects, and (100) and (111) surfaces. For determining the point defect energy values, we have considered a

TABLE III. Comparison of various potentials for Si (all simulation values are reported at the melting point of the respective potential model).

	MEAM[a]	SW[b]	Tersoff-4[c]	Tersoff-ARK[c]	Expt.
Melting point (K)	1475	1691	2509	1711	1687[d]
Density of liquid ($g\ ml^{-1}$)	2.302	2.459	2.225	2.589	2.583[e]
Heat of fusion at melting ($kJ\ mol^{-1}$)	35.0	30.9	39.7	19.3	50.6[b]
C_P of liquid ($J\ mol^{-1}\ K^{-1}$)	32.3	35.3	~38.5	~31.0	29.2[b]
Liquid coordination number	6.0–8.2	5.5–6.2	~4.7	~5.4	~6.4[b]

[a]Data taken from Ref. 23.
[b]Data taken from Ref. 53.
[c]Present work.
[d]Data taken from Ref. 49.
[e]Data taken from Ref. 50.

system of 216 atoms with the periodic boundary conditions and have added or subtracted one atom to make it an interstitial defect or vacancy. The system is allowed to relax before computing the energy. For a comparison, the point defect energy values computed by Tersoff[3] on the Tersoff-3 potential and the recent density functional theory (DFT) results given by Goedecker *et al.*[54] and Leung *et al.*[55] are also listed in the table.

From the data listed in Table IV, we note that the values of the vacancy energy given by Tersoff-3, Tersoff-4, and Tersoff-ARK are equal and are comparable to that obtained by Goedecker *et al.*[54] under the local density approximation (LDA). We also note that the tetrahedral interstitial energy value given by the Tersoff-4 potential is ~14% higher and that by the Tersoff-ARK potential is ~36% lower than the corresponding LDA value determined by Leung *et al.*[55] As regards the hexagonal interstitial energy, the value given by the Tersoff-4 potential is ~39% higher and that by the Tersoff-ARK potential is ~15% lower than the corresponding LDA value given by Leung *et al.* It may also be noted that the value of the hexagonal interstitial energy given by the Tersoff-ARK potential is in excellent agreement with the corresponding LDA value determined by Goedecker *et al.*[54]

TABLE IV. Point defect and surface energy values.

	Tersoff-3	Tersoff-4	Tersoff-ARK	Other
Point defect energy (eV)				
Vacancy	3.7[a]	3.7	3.7	3.17,[b] 3.56[c]
Interstitial (tetrahedral)	3.8[a]	3.9	2.2	3.43[d]
Interstitial (hexagonal)	4.7[a]	4.6	2.8	3.31[b,d] 2.87[c]
Surface energy ($eV/Å^2$)				
Si(100)	0.144[e]	0.144	0.142	
Si(111)	0.080[e]	0.080	0.078	

[a]Reference 3.
[b]Reference 54; DFT calculation using general gradient approximation (GGA).
[c]Reference 54; DFT calculation using LDA.
[d]Reference 55.
[e]Reference 39.

To compare the surface energy values with the present results for the Tersoff-4 and Tersoff-ARK potentials, we have included the results of Balamane *et al.*[39] for the Tersoff-3 potential for Si(100) and Si(111) surfaces in Table IV. We note that the surface energy values given by the Tersoff-4 potential are equal to the corresponding values given by the Tersoff-3 potential, and the values given by the Tersoff-ARK potential are ~2% lower. It may be noted that all six values listed in the table for surface energy correspond to the ideal unrelaxed configuration.

The agreement between the Tersoff-4 and Tersoff-ARK potentials in predicting surface energy as well as vacancy energy, as listed in Table IV, again shows that the Tersoff-4 and Tersoff-ARK potentials give nearly the same results when the deformation in the bond angles and bond lengths is small. The higher values of hexagonal interstitial energy as well as tetrahedral interstitial energy given by the Tersoff-4 potential show that as compared to the Tersoff-ARK potential, the Tersoff-4 potential makes the deformation more difficult; qualitatively, this observation is consistent with the fact that the melting point given by the Tersoff-4 potential is higher than that given by the Tersoff-ARK potential.

e. Other points. Figure 10 compares the radial distribution function (RDF) of liquid Si at 3000 K given by V_V (solid curve) and V_{IV} (dotted curve). Table V compares the locations of the first and next peaks, the height of the first peak, and the full width at half maximum (FWHM) of the first peak. For comparison, the values given in Ref. 3 for V_{III} and those given by the experiment[56,57] are also reported in the table. We note that there is a good agreement among all four sets of numbers.

The coordination number for the solid crystal, given by V_{IV} as well as V_V, is found to be 4.0, which is in agreement with the tetrahedral structure. For the liquid, however, we

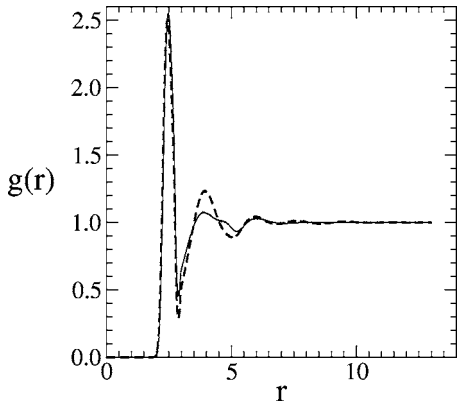

FIG. 10. The RDF for liquid Si at 3000 K: solid curve for the Tersoff-ARK potential and dotted curve for the Tersoff-4 potential.

note that the coordination number ~5.4, given by V_V, which is higher than the value ~4.7 given by V_{IV} but is lower than the experimental value ~6.4 (see Table III).

Keblinski *et al.*[58] remark that with the exception of the Stillinger and Weber (SW) potential[5] and a similar potential developed by Mistriotis *et al.*,[21] among more than 30 empirical potentials for silicon, no potential other than the environmental-dependent interatomic potential (EDIP) developed by Justo *et al.*[16] predicts a reasonable melting point. Recently, there has been a number of studies on the computation of the melting point of Si using the potential of Justo *et al.* The melting point given by this potential is found to be 1572 K by Kaczmarski *et al.*,[59] 1582±25 K by Miranda and Antonelli,[60] and 1520±30 K by Keblinski *et al.*,[58] all within 10% of the experimental value, 1687 K. For comparison, the value of the melting point given by the Tersoff-ARK potential is 1711 K. With respect to the heat of fusion and density, the EDIP potential gives[59] a heat of fusion equal to 36.0 kJ mol^{-1} and, contrary to the experiment, it predicts[59] a decrease in density of Si as it undergoes the phase transition from the solid phase to the liquid phase.

It would be interesting to compare various properties of liquid silicon as predicted by the Tersoff-4,[4] Tersoff-ARK, modified-embedded-atom-method (MEAM),[8,23] and Stillinger and Weber (SW) potentials[5] (see Table III for details). First, we note that none of these models, including Tersoff-ARK, provides very good agreement of all the properties listed with the experimental values. Second, compared to the Tersoff-4 potential, Tersoff-ARK yields better agreement with experiment of the melting point, density of the liquid, and specific heat of the liquid. Third, presently, Tersoff-ARK's shortcomings are the prediction of lower values of heat of fusion and liquid coordination number. Both MEAM and SW models give better agreement of the heat of fusion and liquid coordination number with the experiment compared to Tersoff-ARK, but at the expense of the density of liquid (and the melting point in the case of MEAM). Also, MEAM and SW models predict specific heat of the liquid nearly 10% and 20% higher than the experiment, respectively. With respect to the solid, the computed results are expected to be nearly the same for the Tersoff-4 and Tersoff-ARK potentials when the temperature is not high and the structure remains tetrahedral. Future studies will focus on further modification of the parameters in the Tersoff-ARK potential, such that these two properties as well as other properties, such as elastic constants and phonon frequencies, agree with the values reported in the literature. This may involve modification of the numerical values of some of the parameters in the Tersoff's potential and/or functional modification of the parameters such that a majority of experimental values agree with predictions.

TABLE V. A comparison of RDF results given by different potentials with the experiment.

	V_V[a]	V_{IV}[b]	V_{III}[c]	Experiment
Location of the first peak (Å)	2.48	2.44	2.45	2.5,[d] 2.41–2.46[e]
Location of the next peak (Å)	3.88	3.95	3.90	3.8,[d] 3.28–3.45[e]
FWHM of first peak (Å)	0.48	0.48	0.52	0.6[d]
Height of the first peak	2.55	2.50	2.4	2.5[d]

[a]Present modification.
[b]Tersoff-4 potential as given in Ref. 4.
[c]Reference 3.
[d]Reference 56.
[e]Reference 57.

IV. SUMMARY AND CONCLUSIONS

The void-nucleated melting method has been employed to compute the melting point of Si using the Tersoff-4 potential. The good agreement of the computed melting point to that determined by Yoo *et al.*[24] by the method of equilibration of coexisting solid and liquid phases using the same potential supports the appropriateness of the void-nucleated method, which is at present empirical.

The computed value of the ratio of the melting point and mechanical melting point f, given by Eq. (1), is found to be 0.82. This value of f is comparable to those computed for van der Waals and molecular crystals of Ar, Ne, CH_3NO_2, RDX, TNAZ, ammonium nitrate, and ammonium dinitramide as well as those given by the theoretical model of Lu and Li[33] for a large number of metallic crystals of Al, Au, Co, Cu, Fe, Mn, Ni, Pb, Pd, Pt, Sb, and Sn; for all these crystals, f is found to be in the range 0.77 to 0.85.

The validity of the void-nucleated melting method and the fact that $f \sim 0.8$ for a large number of systems suggests the need for a more rigorous investigation on whether the existence of the plateau region in the void size versus melting temperature is universal, whether the melting point in the plateau region corresponds to the thermodynamic melting point, and whether the value of $f \sim 0.8$ is also a universal result.

In agreement with the previous computed results, the present studies show that the Tersoff-4 potential overestimates the melting point by more than 50% and gives the density of the liquid ~14% lower than the experiment. It is also noted that an addition of a long-range Lennard-Jones (12-6) interaction to the Terosoff-4 potential does not significantly change the melting point.

The present studies also show that a simple modification in 3 of the 12 parameters of the Tersoff-4 potential can bring

the melting point as well as the density of the liquid into good agreement with experiment without altering the density and energy values of the solid crystal at room temperature.

A comparison of density over a wide range of temperatures shows that the density of the solid predicted by the Tersoff-ARK potential (Tersoff potential with the modified parameters) is larger than that given by the Tersoff-4 potential. This difference is not appreciable at room temperature, but increases with temperature and is $\sim 1\%$ at the melting point. The computed cohesive energy of the solid, the point defect energy corresponding to a vacancy, and the surface energy values for (100) and (111) surfaces are also found to be almost equal for the modified as well as unmodified parameters. The point defect energy values corresponding to the hexagonal and tetrahedral interstitials, however, are found to be $\sim 40\%$ lower when the modified parameters are used. The hexagonal interstitial energy given by the modified parameters is found to be in excellent agreement with the corresponding LDA value determined by Goedecker *et al.*[54] The coordination number of the liquid and specific heat are also found to be in better agreement with experiment when the modified set of parameters is used. It may be of interest to investigate further to see if the Tersoff-ARK potential is a better choice for other properties, such as elastic constants and phonon frequencies.

ACKNOWLEDGMENTS

This project is funded by Grant Nos. DMI-0200327 and DMI-0457663 from the National Science Foundation. We thank Dr. W. DeVries, Dr. G. Hazelrigg, Dr. J. Cao, and Dr. D. Durham of the Division of Design, Manufacturing, and Industrial Innovation; Dr. B. M. Kramer, Engineering Centers Division; and Dr. J. Larsen Basse, Tribology and Surface Engineering program for their interest and support of this work. This project was also funded by a DEPSCoR grant on the Multiscale Modeling and Simulation of Material Processing (Grant No. F49620-03-1-0281). The authors thank Dr. Craig S. Hartley of the AFOSR for his interest in and support of this work. One of the authors (R.K.) also thanks A. H. Nelson, Jr., Endowed Chair in Engineering, for additional support for this project.

*Corresponding author. Fax: (405) 744-7873; Email address: ranga@ceat.okstate.edu

[1] J. Tersoff, Phys. Rev. Lett. **56**, 632 (1986).
[2] J. Tersoff, Phys. Rev. B **37**, 6991 (1988).
[3] J. Tersoff, Phys. Rev. B **38**, 9902 (1988).
[4] J. Tersoff, Phys. Rev. B **39**, 5566 (1989).
[5] F. H. Stillinger and T. A. Weber, Phys. Rev. B **31**, 5262 (1985); Phys. Rev. B **33**, 1451(E) (1986).
[6] G. Ackland, Phys. Rev. B **40**, 10351 (1989).
[7] C. F. Abrams and D. B. Graves, J. Appl. Phys. **86**, 5938 (1999).
[8] M. I. Baskes, J. S. Nelson, and A. F. Wright, Phys. Rev. B **40**, 6085 (1989).
[9] D. W. Brenner and B. J. Garrison, Phys. Rev. B **34**, 1304 (1986); P. M. Agrawal, L. M. Raff, and D. L. Thompson, Surf. Sci. **188**, 402 (1987).
[10] R. Biswas and D. R. Hamann, Phys. Rev. Lett. **55**, 2001 (1985); Phys. Rev. B **36**, 6434 (1987).
[11] B. C. Bolding and H. C. Andersen, Phys. Rev. B **41**, 10568 (1990).
[12] A. E. Carlsson, P. A. Fedders, and C. W. Myles, Phys. Rev. B **41**, 1247 (1990).
[13] J. R. Chelikowsky, J. C. Phillips, M. Kamal, and M. Strauss, Phys. Rev. Lett. **62**, 292 (1989).
[14] B. W. Dodson, Phys. Rev. B **35**, 2795 (1987).
[15] D. Humbird and D. B. Graves, J. Chem. Phys. **120**, 2405 (2004).
[16] J. F. Justo, M. Z. Bazant, E. Kaxiras, V. V. Bulatov, and S. Yip, Phys. Rev. B **58**, 2539 (1998).
[17] E. Kaxiras and K. C. Pandey, Phys. Rev. B **38**, 12736 (1988).
[18] P. Keblinski, M. Z. Bazant, R. K. Dash, and M. M. Treacy, Phys. Rev. B **66**, 064104 (2002).
[19] K. E. Kho and S. Das Sarma, Phys. Rev. B **38**, 3318 (1988).
[20] P. N. Keating, Phys. Rev. **145**, 637 (1966); W. Weber, Phys. Rev. B **15**, 4789 (1977).
[21] A. D. Mistriotis, N. Flytzanis, and S. C. Farantos, Phys. Rev. B **39**, 1212 (1989).
[22] E. Pearson, T. Takai, T. Halicioglu, and W. A. Tiller, J. Cryst. Growth **70**, 33 (1984).
[23] S. J. Cook and P. Clancy, Phys. Rev. B **47**, 7686 (1993).
[24] S. Yoo, X. C. Zeng, and J. R. Morris, J. Chem. Phys. **120**, 1654 (2004).
[25] J. Solca, A. J. Dyson, G. Steinebrunner, and B. Kirchner, Chem. Phys. **224**, 253 (1997).
[26] P. M. Agrawal, B. M. Rice, and D. L. Thompson, J. Chem. Phys. **118**, 9680 (2003).
[27] Z. H. Jin, P. Gumbsch, K. Lu, and E. Ma, Phys. Rev. Lett. **87**, 055703 (2001).
[28] J. Solca, A. J. Dyson, G. Steinebrunner, B. Kirchner, and H. Huber, J. Chem. Phys. **108**, 4107 (1998).
[29] F. Lutsko, D. Wolf, S. R. Phillpot, and S. Yip, Phys. Rev. B **40**, 2841 (1989).
[30] P. M. Agrawal, B. M. Rice, and D. L. Thompson, J. Chem. Phys. **119**, 9617 (2003).
[31] G. F. Velardez, S. Alavi, and D. L. Thompson, J. Chem. Phys. **120**, 9151 (2004).
[32] G. F. Velardez, S. Alavi, and D. L. Thompson, J. Chem. Phys. **119**, 6698 (2003).
[33] K. Lu and Y. Li, Phys. Rev. Lett. **80**, 4474 (1998).
[34] S. R. Phillpot, J. F. Lutsko, D. Wolf, and S. Yip, Phys. Rev. B **40**, 2831 (1989).
[35] C-S. Zha, R. Boehler, D. A. Young, and M. Ross, J. Chem. Phys. **85**, 1034 (1986).
[36] J. R. Morris and X. J. Song, Chem. Phys. **116**, 9352 (2002); J. R. Morris, C. Z. Wang, K. M. Ho, and C. T. Chan, Phys. Rev. B **49**, 3109 (1994).
[37] A. Gavezzotti, J. Mol. Struct. **485-486**, 485 (1999).
[38] P. M. Agrawal, B. M. Rice, and D. L. Thompson (unpublished).
[39] H. Balamane, T. Halicioglu, and W. A. Tiller, Phys. Rev. B **46**, 2250 (1992).

[40] M. P. Allen and D. J. Tildesley, *Computer Simulation of Liquids* (Oxford Science Publications, Oxford, UK, 1993).
[41] S. Melchionna, G. Ciccotti, and B. L. Holian, Mol. Phys. **78**, 533 (1993).
[42] F. A. Lindemann, Phys. Z. **11**, 609 (1910); J. J. Gilvarry, Phys. Rev. **102**, 308 (1956).
[43] M. Born, J. Chem. Phys. **7**, 591 (1939); Proc. Cambridge Philos. Soc. **36**, 160 (1940).
[44] L. Burakovsky, D. L. Preston, and R. R. Silbar, J. Appl. Phys. **88**, 6294 (2000).
[45] L. Burakovsky, D. L. Preston, and R. R. Silbar, Phys. Rev. B **61**, 15011 (2000).
[46] L. Burakovsky and D. L. Preston, Solid State Commun. **115**, 341 (2000).
[47] L. Gómez, A. Dobry, and H. T. Diep, Phys. Rev. B **63**, 224103 (2000).
[48] A. K. Rappe, C. J. Casewit, K. S. Colwell, W. A. Goddard III, and W. M. Skiff, J. Am. Chem. Soc. **114**, 10024 (1992).
[49] D. R. Lide, editor-in-chief, *CRC Handbook of Chemistry and Physics* (CRC Press, Boca Raton, FL, 2004–2005).
[50] Z. Zhou, S. Mukherjee, and W. Rhim, J. Cryst. Growth **257**, 350 (2003).
[51] I. Barin and O. Knacke, *Thermodynamic Properties of Inorganic Substances* (Springer-Verlag, Berlin, 1973).
[52] M. W. Chase, Jr., C. A. Davies, J. R. Downey, Jr., D. J. Frurip, R. A. McDonald, and A. N. Syverud, J. Phys. Chem. Ref. Data Suppl. **14**, 1 (1985).
[53] J. Q. Broughton and X. P. Li, Phys. Rev. B **35**, 9120 (1987).
[54] S. Goedecker, T. Deutsch, and L. Billard, Phys. Rev. Lett. **88**, 235501 (2002).
[55] W. K. Leung, R. J. Needs, G. Rajagopal, S. Itoh, and S. Ihara, Phys. Rev. Lett. **83**, 2351 (1999).
[56] Y. Waseda and K. Suzuki, Z. Phys. B **20**, 339 (1975).
[57] S. Ansell, S. Krishnan, J. J. Felten, and D. L. Price, J. Phys.: Condens. Matter **10**, L73 (1998).
[58] P. Keblinski, M. Z. Bazant, R. K. Dash, and M. M. Treacy, Phys. Rev. B **66**, 064104 (2002).
[59] M. Kaczmarski, R. Rurali, and E. Hernandez, Phys. Rev. B **69**, 214105 (2004).
[60] C. R. Miranda and A. Antonelli, J. Chem. Phys. **120**, 11672 (2004).